E3S Web of Conferences **9**, 10009 (2016)
*E-UNSAT 2016*
DOI: 10.1051/e3sconf/20160910009

# Estimation of hydraulic conductivity function in unsaturated pyroclastic soils

Marianna Pirone[1a], Raffaele Papa[1], Marco Valerio Nicotera[1] and Gianfranco Urciuoli[1]

[1] *University of Naples 'Federico II', Department of Civil, Architectural and Environmental Engineering, Via Claudio 21, 80125 Naples*

**Abstract.** A full understanding of slope failure conditions in unsaturated pyroclastic slope needs a fair analysis of groundwater flow and, therefore, a proper hydraulic soil characterization in terms of either soil water retention curves (SWRC) and hydraulic conductivity function (HCF). A practical method to detect the HCF by processing in situ data is provided, thus, the identification of the HCFs operating on site by applying the Soil Water Balance (SWB) to the pyroclastic soil cover is carried out. In this regard data monitoring (matrix suction and volumetric water content) collected at experimental field of Monteforte Irpino in Southern Italy over four years have been used. Moreover a comparison between the saturated hydraulic conductivity from lab test and from in situ measurements is carried out and the results confirm that the effective hydraulic conductivity operating at the site scale is higher than the hydraulic conductivity obtained in the laboratory for the whole range of suction measured at site.

## 1 Introduction

Flowslides in granular soils undoubtedly constitute a major threat to human life, man made structures and the environment in general. In unsaturated soils, rainfall is the most usual triggering cause, due to rainwater infiltrating into the superficial soil, which causes a decrease in matric suction and consequently in shear strength. In this regard, Early Warning Systems (EWSs) are widely used as measures for rapid landslide risk mitigation and can be set up by using physically-based models able to reproduce the hydro-mechanical slope behaviour through numerical analyses [1], [2]. However the weakness in forecasting rainfall-induced landslides is often due to uncertainties about hydraulic soil characterisation at the site scale [3]. Here a method to detect a hydraulic conductivity function by processing in situ data is provided, in particular, the identification of the HCFs operating on site by applying the Soil Water Balance (SWB) to a pyroclastic soil cover is carried out. These features have been investigated by processing data from the test site at Monteforte Irpino [4] where meteorological data, matric suction and volumetric soil water content measurements were collected for about four years. Moreover the saturated hydraulic conductivity and the hydraulic conductivity function obtained in the laboratory [5] are compared with the unsaturated hydraulic conductivity values derived from in situ measurements to show that laboratory testing results are not always representative of the effective hydraulic conductivity operating at the site scale. Lastly some measurements of saturated hydraulic conductivity gained at site via double ring infiltrometer tests [6] are reported.

[a] Corresponding author: marianna.pirone@unina.it

## 2 Test site

The test site at Monteforte Irpino (40°54'13.11" N, 14°40'24.21"E), about 40 km East of Naples, was selected as being representative of other pyroclastic slopes in Campania subjected to rapid landslides (e.g. Pizzo D'Alvano, Monti di Avella and Monte Partenio). In the test site area, the slope is quite regular and has an average angle of 25–30°, with local values reaching 35–40°. An area of about 230 m$^2$ was chosen on the slope and twenty instrumented vertical sections were set up along three longitudinal alignments, sections A–A', B–B', C–C'. The stratigraphic profile consists of an unsaturated pyroclastic soil cover a few metres thick (3–5.5 m), deposited by a series of eruptions of Mt Somma–Vesuvius on top of the limestone bedrock. The test site was monitored from 2006 to 2012. The monitoring equipment consisted of: (i) 94 traditional vacuum tensiometers, i.e.: jet-fill tensiometers (SoilMoisture Equipment Corp.) and SMS (Soil Measurement system) tensiometer tubes (SDEC France); (ii) 40 TDR (Time Domain Reflectometry) probes 15 cm long; (iii) 6 Casagrande piezometers; (iv) a weather station. The tensiometers were installed at different depths along all the vertical sections, TDR and Casagrande piezometers along the verticals only at the central section, B–B'. However, the test site itself has been extensively described elsewhere; readers can refer to [7] and [4] for further detailed information about the instrumented area.

The simplified mean soil profile obtained from experimental investigation through some trenches and boreholes, mean physical properties (specific gravity $G_s$, porosity $\Phi$, dry soil unit weight $\gamma_d$) and instrumentation installed along the central longitudinal section, B–B', of the test site are reported in Figure 1.

To apply the water balance calculation to soil cover, the data collected from the verticals located at the central section, B–B', will be used and reference will henceforth be made to a simplified mean soil profile of three layers of ash soils separated by two pumiceous layers (soils 3 and 5): the superficial ash layer comprises soils 1 and 2; the intermediate ash layer consists of soil 4; the deep ash layer contains soils 6 and 8 (Figure 1).

## 3 Hydraulic conductivity functions

### 3.1. Determination from laboratory tests

Nicotera et al. (2010), [5], presented saturated hydraulic conductivity determined in the laboratory by constant head hydraulic conductivity tests and hydraulic conductivity functions determined by inverse modelling of a sequence of testing phases (i.e. a constant head permeation test, a forced evaporation test, and finally a drying test in a pressure plate apparatus to be conducted on a single undisturbed soil sample) for all the ash soils recovered at the test site. The saturated hydraulic conductivities measured for each soil and the mean values of the parameters of the Mualem–van Genuchten [8] equation modeling the soil water retention curves along main drying paths obtained in the laboratory for each soil are summarized in Table 1 (volumetric water content at saturation, residual volumetric water content, α, n, $l$ Mualem–van Genuchten parameters, $k^{sat}$ ). In Figure 2 the saturated hydraulic conductivity and the hydraulic conductivity function on the plane k (conductivity)-θ (volumetric water content) are reported for ash soils, 1-2, 4, 6 and 8. The saturated hydraulic conductivity measurement decrease from the ground surface to the bottom of soil cover (starting from soils 1&2 to 8). Indeed at fixed interval of volumetric water content, i.e. 0.3 to 0.5, the largest range of the hydraulic conductivities is observed in the surficial soils [9].

According to the literature [10]-[11], measurements of hydraulic conductivity are approximately log-normally distributed. Here the lognormal distribution is applied to the lab measurements of saturated hydraulic conductivity for ash soils (see Figure 4); the number of determinations (N), the standard deviation, σ, of the logarithm of measurements, and the modal and median values resulting from the distribution are reported in Table 2.

Moreover the hydraulic conductivity functions corresponding to median value of saturated hydraulic conductivity from lab tests are reported for ash soils in Figure 3a-d (grey lines).

### 3.2 Determination from in situ measurements

The procedure to estimate the hydraulic conductivity function exploits the in situ measurements of volumetric water content and matric suction collected during autumn and uses the assessment of soil water balance (SWB). By assuming the monitored section of slope as infinite [3], the SWB can be applied to the one-dimensional simplified soil profile comprising all the soil layers along the direction normal to the slope surface (Figure 1) and written as (modified from [12]):

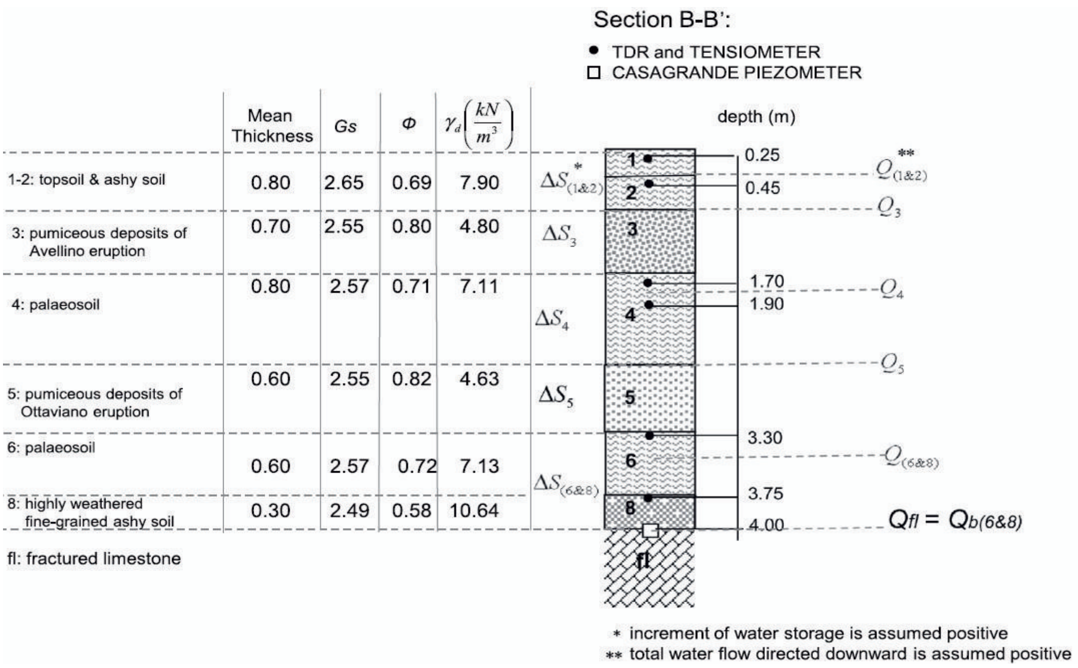


**Figure 1.** Simplified soil profile with mean soil physical properties and the layout of the instrumentation installed along each monitored vertical section along section B–B'. The symbols used to indicate soil water volume storage and groundwater flow in each layer are reported: ΔS water storage variation, $Q_i$ flow through layer i (modified from [3]).

 DOI: 10.1051/e3sconf/20160910009

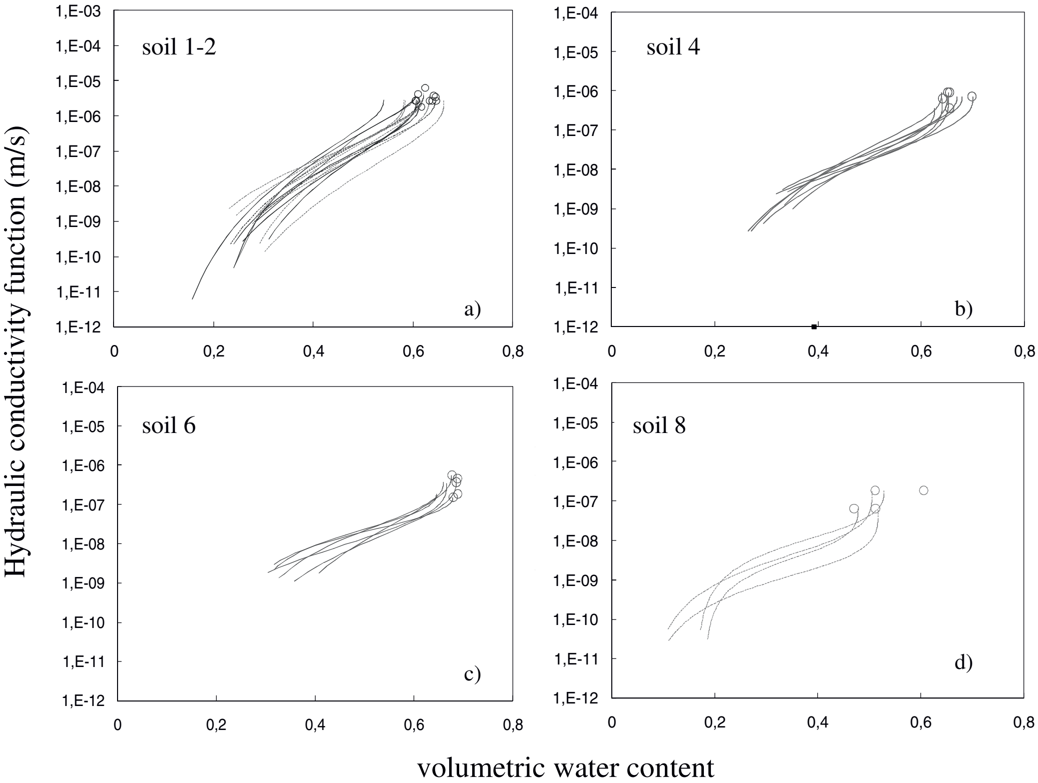


**Figure 2.** Hydraulic conductivity function (continous line) and hydraulic saturated permeability (symbol) obtained in the laboratory on samples from soil 1-2 (a); soil 4(b); soil 6(c); soil 8(d) [5].

$$I - ET_C = \sum_{i=1}^{n_L} \Delta S_i + Q_{fl} \quad (1)$$

$$I - ET_C = Q_{1\&2} \quad (2)$$

where I is the infiltration, $ET_C$ the crop evapotraspiration [13], $\Delta S_i$, the variation in soil water storage in the i-th layer (the superficial, intermediate and deep ash layers being denoted by, respectively, 1 & 2, 4 and6 & 8), $Q_{fl}$ is the water exchange between the entire soil cover and the fractured limestone bedrock, $n_L$ is the number of layers within the soil cover, $Q_{1\&2}$ is the amount of water flowing normal to the slope surface across the top boundary of the superficial ash layer. The physical quantities involved in the SWB are also summarized in Figure 1.

**Table 1** Parameters of Mualem van Genucthen model.

| | **θs** | **θr** | **α (kPa$^{1}$)** | **n** | **l** | **$k_{sat}$ (m/s)** |
|---|---|---|---|---|---|---|
| **1** | 0.565 | 0.135 | 8.08 | 1.716 | -1.052 | $2.13\times10^{-6}$ |
| **2** | 0.617 | 0.143 | 8.72 | 1.602 | -1.054 | $3.04\times10^{-6}$ |
| **4** | 0.659 | 0.164 | 9.30 | 1.495 | -2.850 | $6.85\times10^{-7}$ |
| **6** | 0.669 | 0.198 | 13.10 | 1.645 | -2.698 | $3.08\times10^{-7}$ |
| **8** | 0.508 | 0.120 | 12.20 | 1.390 | -5.707 | $1.08\times10^{-7}$ |

According to [3] it is reasonable to assume that $Q_{fl}$ is exactly zero during October (when the soil groundwater flow into deeper layers was parallel to the slope) and approximately zero during November and December (when the normal flux $Q_{6\&8}$ was just sufficient to provide a moderate variation of the water volume storage in the deeper layers). As a consequence of these observations, in these three months, the amount, $Q_{1\&2j}$, of water flowing normal to the slope surface across the top boundary of the superficial ash layer along the jth vertical section in the time interval from t to t + Δt can be calculated as the volume of water needed to supply the water storage in the whole soil cover during the time interval Δt. Thus eqs. (1)-(2) applied at each single instrumented vertical j-th become:

$$Q_{1\&2j} = \sum_{i=1}^{n_L} \Delta S_{ij} \quad (3)$$

where

$$\Delta S_{ij} = \lfloor S_{ij}(t+\Delta t) - S_{ij}(t) \rfloor \quad (4)$$

For each layer i and vertical profile j, $S_{ij}(t)$ is calculated as the difference between the volumetric soil water contents $\theta_{ij}(t)$ and $\theta_{ij}(0)$ measured respectively at time t and at the beginning of monitoring, multiplied by the thickness of the layer $d_{ij}$ (i.e. assuming that the soil water content is uniform along the layer, [4]):

$$S_{ij} = \lfloor \theta_{ij}(t) - \theta_{ij}(0) \rfloor \cdot d_{ij} \quad (5)$$

DOI: 10.1051/e3sconf/20160910009

Therefore, the fluxes crossing the top of the k-th soil layer at the jth vertical section can be written trivially as:

$$Q_{kj} = \sum_{i=k}^{n_L} \left[ S_{ij}(t+\Delta t) - S_{ij}(t) \right] \tag{6}$$

Thus the mean value of the current hydraulic conductivity for the k-th soil layer at the jth vertical section during the time interval from t to t + Δt can be estimated from measurements of volumetric water content as:

$$k_{kj} \approx -\frac{1}{i_{kj}^{n}} \cdot \frac{Q_{kj}}{\Delta t} \tag{7}$$

However, the ground water flux infiltrating into the limestone may not always be zero in November and December and the distribution of volumetric water content along the first 0.25 m is not always uniform as is assumed instead for the calculation of water volume storage [3]. Thus, the total amount of water flowing across the k-th layers may exceed $Q_{kj}$ obtained from Eq. (6), and hence Eq. (7) provides only a lower estimate for the actual value of hydraulic conductivity. However in [3], it is shown the lower estimate of hydraulic conductivity function matches the upper one proving the robustness of the method proposed here.

Mean values of hydraulic conductivity were calculated for each vertical profile and for each sampling day between October and December. These calculations were performed for: the superficial ash layer comprising soils 1 and 2, $k_{1\&2,j}$; the intermediate ash layer consisting of soil 4, $k_{4,j}$; and the deep ash layer comprising soils 6 and 8, $k_{6\&8,j}$. The calculated values of $k_{kj}$ are plotted in Fig. 3a–d (black-filled symbols) against the corresponding mean volumetric water content.

For all ash soils apart from soil 6, the values of unsaturated hydraulic conductivity estimated from in situ measurements lie above the hydraulic conductivity curve

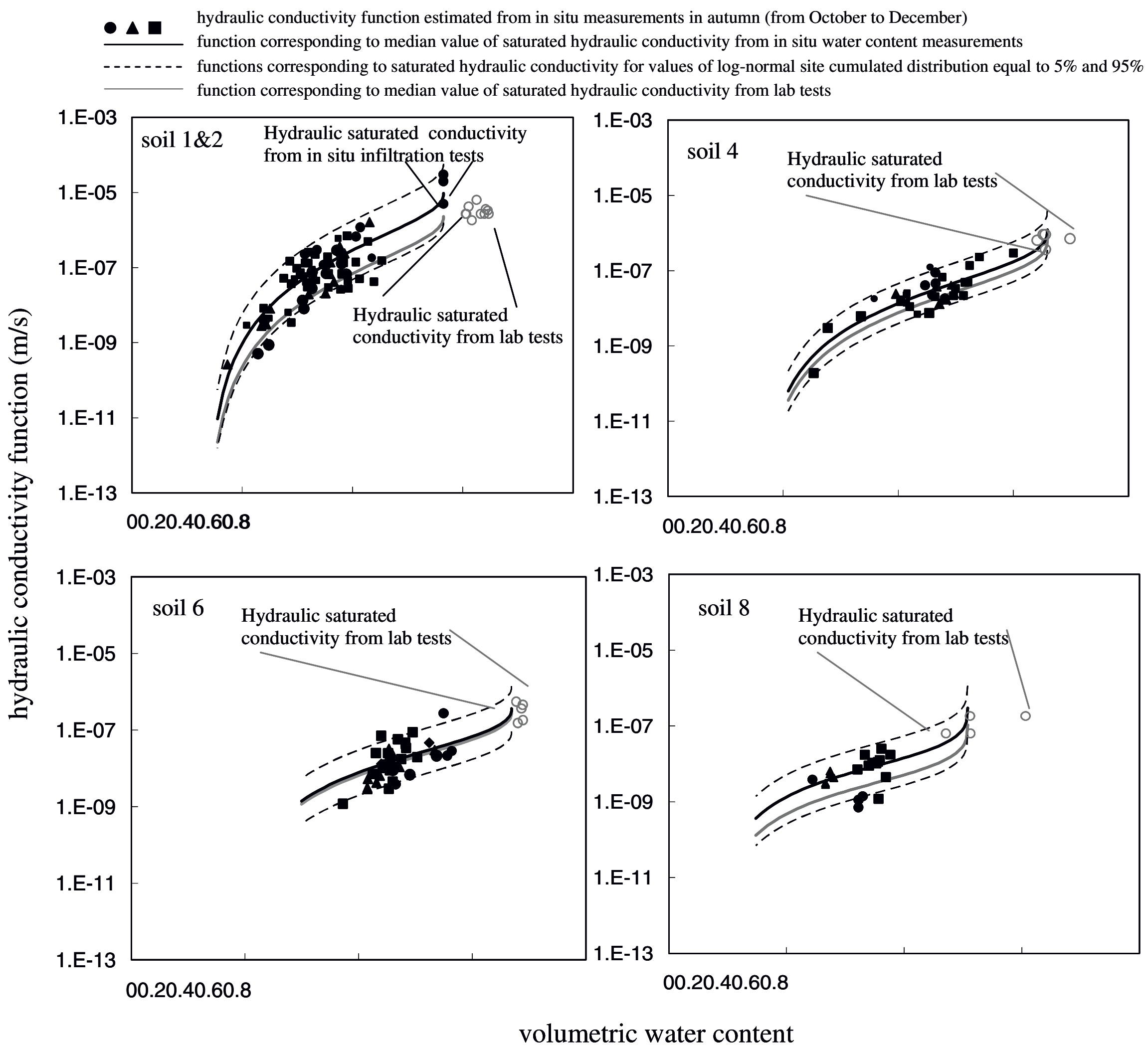


**Figure 3.** Hydraulic conductivity of the ash soils: saturated hydraulic conductivities from lab tests (grey circles) and in situ infiltration tests (black circles); unsaturated hydraulic conductivities determined from in situ measurements of soil water content via Eq. (7)(black symbols), hydraulic conductivity functions estimated on the basis of laboratory tests (grey line) and in situ measurements (black line).

determined in the laboratory, likely due to a poor representativeness of the soil laboratory sample [14]-[15]-[16], to all the uncertainties related to the estimation of in situ permeability and to the presence of some cracks on the soil surface where vegetation is lacking. By observing Fig. 3a–d (black-filled symbols), the variability of $k_{kj}$ derived from field data, evaluated at constant volumetric water content, ranges between 0.5 and 1.5 orders of magnitude. The largest variability results in the surficial layers where ground–atmosphere interaction occurs and local topographic irregularities can affect the hydraulic soil behaviour. Nevertheless, the data from in-situ measurements appear to follow the same shape as the conductivity functions determined in the laboratory, albeit simply shifted towards higher hydraulic conductivity values, especially in the superficial soils for which more data are available. In order to elaborate a log-normal distribution also from in situ measurements, a unique value $k^{sat}_{kj}$ of the saturated hydraulic conductivity of the $k_{th}$ soil layer at the $j_{th}$ vertical is estimated for each $k_{kj}$ data point collected in situ and reported in Fig. 3a–d; $k^{sat}_{kj}$ was calculated by imposing that the curve from the Mualem–van Genuchten model with the shape parameters fixed at the mean values from the lab and the saturated hydraulic conductivity at the chosen value of $k^{sat}_{kj}$ could best fit the data points in hand. In Table 2 the parameters of the log-normal distributions of $k^{sat}_{kj}$ thus obtained are compared to those of the laboratory measurements. In this regard it is worth noting that the median value of the log-normal distribution of hydraulic conductivity from in situ measurements always exceeds that of hydraulic conductivity measured in the laboratory: their ratio is 4 for soils 1 and 2, 2 for soil 4, 1.2 for soil 6, and 3 for soil 8 (see also Figure 4). Therefore, in Fig. 3a–d the continuous black line represents a *reasonable hydraulic conductivity function operative at the site*, obtained through the Mualem–van Genuchten model with a saturated hydraulic conductivity equal to the median value of log-normal distribution of values estimated from in situ measurements and the shape parameters fixed at the mean values obtained from the laboratory tests.

**Table 2** Statistical parameters of log-normal distribution of saturated hydraulic conductivities.

| Soil | method | N (#) | σ (m/s) | $\overline{\mu}$ (m/s) | mode (m/s) | median (m/s) |
|---|---|---|---|---|---|---|
| 1&2 | Lab | 10 | 0.94 | 2.9E-06 | 9.0E-07 | 2.3E-06 |
| | Site | 73 | 1.04 | 1.6E-05 | 2.7E-06 | 9.6E-06 |
| 4 | Lab | 5 | 0.39 | 7.2E-07 | 6.0E-07 | 6.8E-07 |
| | Sito | 36 | 0.75 | 1.6E-06 | 6.2E-07 | 1.2E-06 |
| 6 | Lab | 5 | 0.56 | 3.4E-07 | 2.2E-07 | 3.0E-07 |
| | Site | 36 | 0.83 | 5.2E-07 | 1.9E-07 | 3.6E-07 |
| 8 | Lab | 4 | 0.60 | 1.2E-07 | 7.0E-08 | 1.1E-07 |
| | Site | 21 | 0.99 | 4.20E-07 | 1.1E-07 | 3.00E-07 |

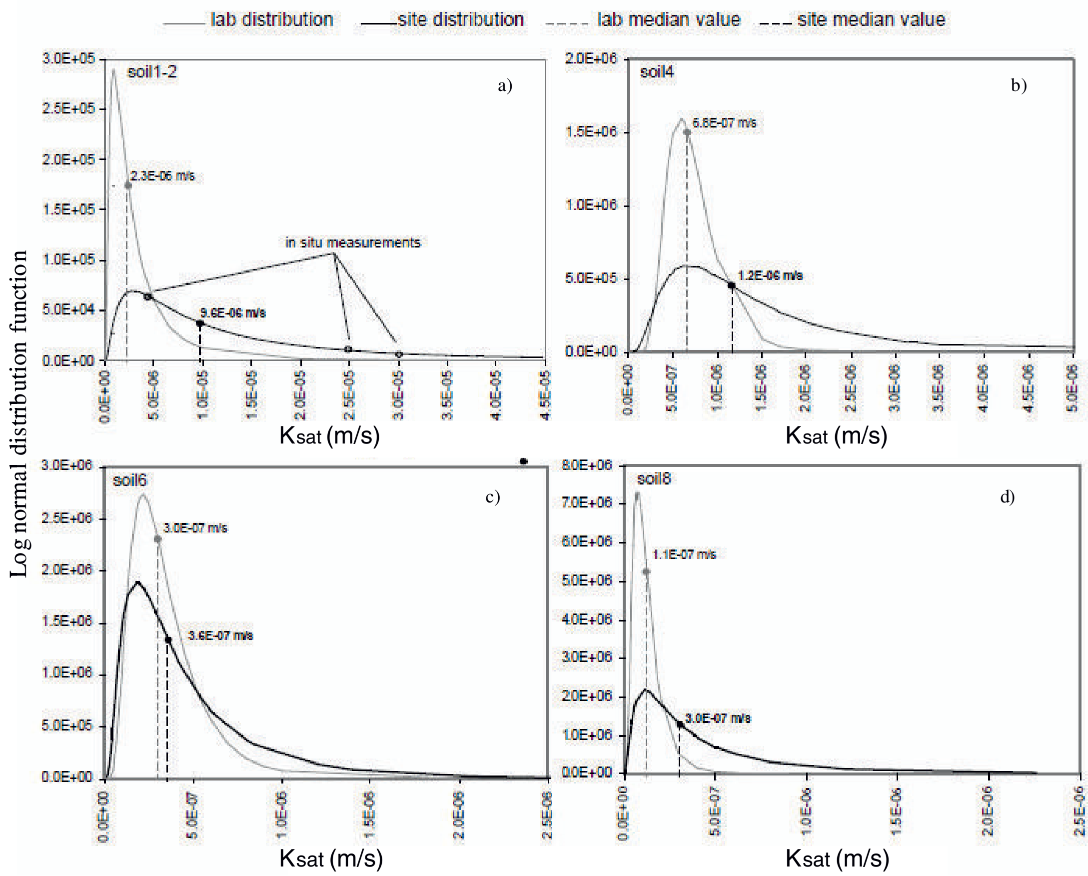


**Figure 4.** Log-normal distribution functions of saturated hydraulic permeability measured in the laboratory and estimated in situ for soil 1-2 (a); soil 4 (b); soil 6 (c); soil8 (d).

**Table 3** Values of saturated conductivity estimated via different methods for each ash soil (modified from [3])

| Soil | method | description | $K_{sat}$ ($10^{-7}$m/s) |
|---|---|---|---|
| 1&2 | in lab measurements | Range between the minimum and maximum measurements | 1.82-63.7 |
| | estimation from in situ measurements | Range between the values corresponding to the cumulative log-normal distribution of 5% and 95% | 15.80- 580 |
| | in situ infiltration tests | Range between the minimum and maximum measurements | 50.00-300 |
| 4 | in lab measurements | Range between the minimum and maximum measurements | 3.64-9.08 |
| | estimation from in situ measurements | Range between the values corresponding to the cumulative log-normal distribution of 5% and 95% | 3.40-41.00 |
| 6 | in lab measurements | Range between the minimum and maximum measurements | 1.52-5.47 |
| | estimation from in situ measurements | Range between the values corresponding to the cumulative log-normal distribution of 5% and 95% | 0.92-14.00 |
| 8 | in lab measurements | Range between the minimum and maximum measurements | 0.64-1.82 |
| | estimation from in situ measurements | Range between the values corresponding to the cumulative log-normal distribution of 5% and 95% | 0.58-15.00 |

### 3.3 In situ measurements of saturated hydraulic conductivity

Some direct measurements of saturated hydraulic conductivity obtained in situ via double ring infiltrometer tests [6] confirm, at least for the shallower soil layer, that the saturated hydraulic conductivity is higher in situ than in the laboratory (see Fig. 3a, black circles). However, the range of the saturated conductivities from infiltration tests contains the median value derived from elaboration of the monitoring data (see Table 2). In Table 3 the range of saturated conductivity determined for each soil and the type of tests performed are summarised. Hence it seems acceptable to perform several in situ measurements of saturated conductivity and some laboratory evaporation tests to obtain the parameters of the Mualem–van Genuchten hydraulic conductivity function operating at the site scale.

## 4 Conclusion

A practical method to set an appropriate hydraulic conductivity function is suggested. It is enough to perform several in situ measurements of saturated conductivity and some evaporation tests in accordance with the procedure proposed by [5] to obtain the parameters to be used in the Mualem–van Genuchten model. As regards the test site, the saturated conductivities estimated from in situ measurements prove higher than those determined in the laboratory, especially for the superficial ash layer, the amplification ratio being 4. Thus the non-representativeness of the laboratory samples was proved.

## References

1. L. Pagano, L. Picarelli, G. Rianna, G. Urciuoli, Landslides **7**, 3, 273–289 (2010)
2. M. Pirone, R. Papa, M.V. Nicotera, G. Urciuoli, Engineering Geology for Society and Territory **2**, Landslide Processes, 1069-1073 (2015)
3. M. Pirone, R. Papa, M.V. Nicotera, G. Urciuoli, Journal of Hydrology **528**, 63–83 (2015)
4. M. Pirone, R. Papa, M.V. Nicotera, G. Urciuoli, Landslides **12**, 2, 259–276 (2015)
5. M.V. Nicotera, R. Papa, G.Urciuoli, Geotech. Test. J. **33**, 4, 263–285 (2010)
6. ASTM D5126-90, Standard Guide for Comparison of Field Methods for Determining Hydraulic Conductivity in the Vadose Zone. doi: 10.1520/D5126-90R04 (2004)
7. R. Papa, M. Pirone, M.V. Nicotera, G. Urciuoli, Geotechnique **63,** 5, 420–426 (2013)
8. M.Th. van Genucthen, Soil Sci. Soc. Am. J. **44**, 892-898 (1980)
9. M. Pirone, R. Papa, M.V. Nicotera, G. Urciuoli, Volcanic Rocks and Soils – Rotonda et al. (eds) © 2016 Taylor & Francis Group, London, ISBN 978-1-138-02886-9, 273-280 (2016)
10. R.J. Hoeksema, P.K. Kitanidis, Water Resour. Res. **21**, 4, 563–572 (1985)
11. E.A. Sudicky, Water Resourc. Res. **22**, 13, 2069–2083 (1986)
12. G.E. Blight, Géotechnique **47**, 4, 715–767 (1997)
13. R.G. Allen, L.S. Pereira, D. Raes, M. Smith, Crop evapotranspiration: Guidelines for computing crop requirements. Irrig. Drain. **56**, FAO, Rome, Italy (1998)
14. R. Greco, L. Comegna, E. Damiano, A. Guida, L. Olivares, L. Picarelli, Earth Syst. Sc. **17**, 10, 4001–4013 (2013)
15. A. Basile, G. Ciollaro, A. Coppola, Water Resour. Res. **39**, 12, 1–12 (2003)
16. M. Pirone, R. Papa, M.V. Nicotera, G. Urciuoli, Procedia Earth Planet. Sci. **9**, 163–170 (2014)

[a] Corresponding author: marianna.pirone@unina.it